RS
4,5

666

Received 20 August 2025
Revised 17 September 2025
Accepted 18 September 2025

Research on earthquake early warning and emergency response for high-speed railways based on the PLUM principle

Kun Gu and Lin Yang
China Academy of Railway Sciences Corporation Limited, Beijing, China
Datian Zhou
School of Electronic Information Engineering, Beijing Jiaotong University, Beijing, China
Nan Xi
China Earthquake Networks Center, Beijing, China, and
Zhongwei Tan
School of Electronic Information Engineering, Beijing Jiaotong University, Beijing, China

Abstract

Purpose – This study aims to design and validate an emergency response method for high-speed railway earthquake early warning (EEW) systems based on the Propagation of Local Undamped Motion (PLUM) principle in order to enhance the timeliness and accuracy of warnings under seismic threats.

Design/methodology/approach – A hierarchical architecture of the railway EEW system was adopted, in which self-built stations along the railway serve as the backbone and the national seismic network provides supplementary data. Warning zones were designed along the railway using overlapping trapezoidal layouts to cover seismic stations and reduce inter-regional time delays. Offline replay experiments were conducted using 82 historical earthquake events and records from 61 seismic stations to evaluate the timeliness and accuracy of warning information.

Findings – The results indicate that the PLUM-based early warning method can issue emergency response information before destructive seismic waves arrive. Multiple earthquake experiments demonstrated high reliability and stability, with effective detection across different magnitudes and epicentral distances. Furthermore, the trapezoidal overlapping zone design improved regional consistency and significantly reduced missed alerts.

Originality/value – This work represents the first systematic application of the PLUM method to high-speed railway EEW in China. By integrating railway operational requirements, the proposed method provides a practical and robust emergency response strategy, offering new insights into seismic risk mitigation for China's high-speed railways.

Keywords High-speed railway safety, Earthquake early warning, PLUM method, Double-trapezoid warning zone, Simulation validation, Emergency response

Paper type Research article

Funding: This work is supported by National Key Project supported by China State Railway Group (No. K2024G008), Sichuan Science and Technology Major Program (No. 2023ZDZX0010), Foundation of China State Railway Group Company Limited (No. Q2024G018), Center of National Sciences Railway Intelligent Transportation System Engineering and Technology (No. RITS2024KF06) and Foundation of China Academy of Railway Sciences Corporation Limited (No. 2024YJ311 and 2024YJ178).

Railway Sciences
Vol. 4 No. 5, 2025
pp. 666-681
Emerald Publishing Limited
e-ISSN: 2755-0915
p-ISSN: 2755-0907
DOI 10.1108/RS-08-2025-0027

1. Introduction to high-speed railways and their earthquake early warning systems

1.1 Development of high-speed railway earthquake early warning systems

The development of earthquake early warning (EEW) systems for high-speed railways in China has undergone two main stages—initiation and development—and is now advancing toward an enhancement stage. This progression has been driven by the emergence of new technological elements, including next-generation communications, sensing, artificial intelligence, and high-performance computing. Under the condition of continuous aggregation of large-scale seismic ground motion data, the system is evolving to deliver faster, more accurate, and more intelligent warning capabilities.

1.1.1 Initiation stage. Following years of tracking and analyzing international experience, China independently developed an EEW system designed to monitor seismic ground motions in areas traversed by high-speed trains. The system utilizes dedicated seismic monitoring stations distributed along the railway lines to detect ground motion anomalies. When abnormal vibrations are detected, corresponding emergency measures can be initiated (Figure 1).

The coverage area of this dedicated seismic monitoring network is linear in configuration, with station locations planned at intervals of 20–30 km along the railway lines. Each station is equipped with a pair of strong-motion seismometers; an alarm is triggered only if both instruments record signals exceeding a preset threshold (Jin, 2021).

1.1.2 Development stage. To ensure the safety of an increasingly extensive high-speed railway network during earthquakes, the EEW system has evolved to a new architecture comprising a central system and field monitoring devices (Yang, Yan, & Guo, 2015; Yan, Yang, & Guo, 2016; Liu, 2019; Yang, Yan, & Zhang, 2021a; Yang, Gong, Gong, Zhou, & Zhang, 2022) (Figure 2). This architecture operates at two tiers: Tier-1 is the Railway Bureau central system; Tier-2 is the field-monitoring layer. The Tier-1 central system acts as the "brain" of the EEW network, responsible for seismic information analysis, processing, and the issuance of train-control commands (Hu, Liu, & Yang, 2016). Specifically, it: (1) provides two warning modes for cross-regional operations—in-place (local) warnings and remote warnings; (2) executes emergency interventions via three pathways; and (3) performs self-correction to mitigate false alarms. Tier-2 field devices are installed along railway lines (Guo, 2016; Hu, 2016) to monitor ground motions, generate warnings/alarms, and transmit them to the central system.

Each Railway Bureau operates a central system that ingests warning/alarm data from field devices and related subsystems, performs integrated analysis (Xi, Wang, & Ma, 2017), rapidly

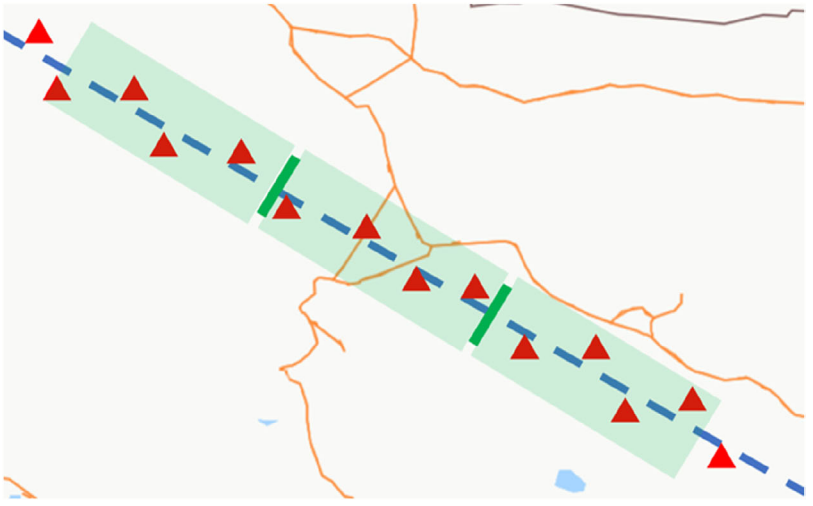

Figure 1. Distribution of dedicated ground-motion monitoring stations. Source(s): Authors' own work

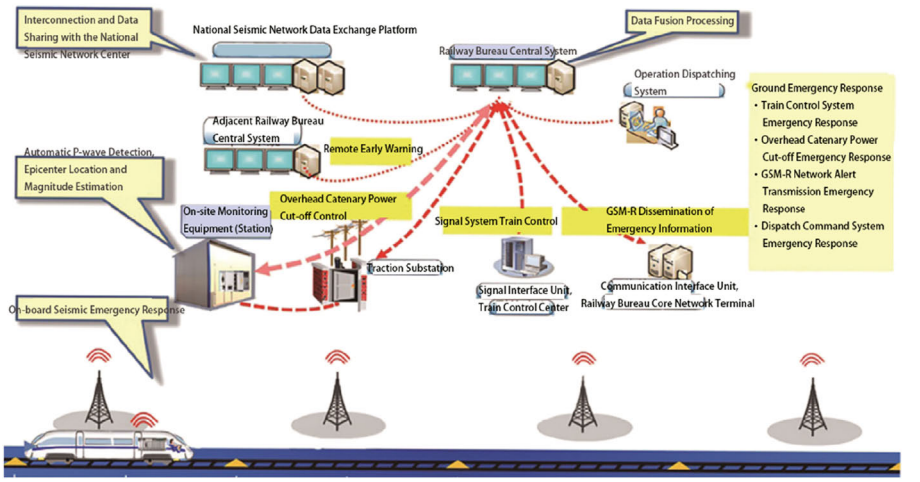

Figure 2. Schematic diagram of the new architecture of the high-speed railway EEW monitoring system. Source(s): Authors' own work

formulates emergency response information (Yang, 2018a, b; Yang, Zhang, & Hu, 2023a), and applies measures according to predefined response levels (Yan, 2017; Liu, Shang, & Feng, 2021). The three intervention pathways are: (1) via the GSM-R network to on-board EEW units for speed restriction or emergency braking; (2) via the seismic-signal interface to trigger the train control system for emergency braking; and (3) via the traction-power interface to actuate the traction power supply for catenary de-energization.

The central system consists of interface servers, emergency-response servers, databases, and corresponding system/application software. Upon an earthquake, it delineates the affected track segments, automatically generates emergency instructions, and dispatches them to the relevant train sets, signal interfaces, and traction-power interfaces to enable rapid response. Notably, the signal and traction interfaces are fixed along the line, whereas train positions are known and time-varying; thus, once the affected lines and extents are determined and response rules applied, rapid operational handling can be achieved.

1.1.3 Enhancement stage. In 2018, China State Railway Group and the China Earthquake Administration signed a renewed strategic cooperation agreement on EEW for high-speed railways. The national seismic network data exchange platform was integrated into the high-speed railway EEW system, enabling seamless interconnection between the railway EEW network and the national seismic network.

With the incorporation of neighboring Railway Bureaus and seismic network information, the EEW system now aggregates multi-source data from the primary line, adjacent lines, neighboring bureaus, and the China Earthquake Network. These include seismic monitoring data, EEW alerts, predicted intensity maps, ground motion parameters, rapid earthquake parameter reports, and alarm signals.

Given the vast amount of data generated by the interconnected high-speed railway network, real-time emergency response also requires data compression to ensure the timeliness of actions (Yang, Liu, & Zhang, 2019; Jiang, Ma, & Ye, 2019; Yang, Zhu, & Zhang, 2023b; Hu & Yang, 2024).

1.2 Opportunities and challenges posed by massive ground-motion observations

In July 2024, the National Earthquake Intensity Rapid Reporting and Early Warning Project passed its acceptance review, achieving dense deployment in key areas and effective coverage

in general areas, with an average inter-station spacing of approximately 13–47 km (China Earthquake Networks Center, 2025). The daily volume of newly acquired raw seismic data can reach the terabyte scale, which exceeds the capacity of traditional computational resources for real-time processing (TDengine, 2023). The availability of massive ground-motion observations is creating unprecedented opportunities for high-speed railway EEW systems, while simultaneously introducing significant technical challenges.

In the future, ultra-dense observation networks—such as node-based dense arrays and submarine fiber-optic arrays—will be capable of capturing finer spatiotemporal details of seismic ground motions. For real-time processing of such massive datasets, next-generation computational frameworks at the second to sub-second level will be required, with the capability to substantially reduce the latency of post-event EEW calculations.

Given considerations of data sovereignty and security, sensitive seismic data may involve issues related to national security and intellectual property, necessitating standardized guidance to balance open sharing and confidentiality review. Furthermore, the heterogeneity of data sources—including variations in instrumentation, sampling rates, file formats, and metadata standards—poses additional challenges for data integration. The field is thus transitioning from an era of "data scarcity" to one of "data abundance." Leveraging these massive ground-motion datasets to enhance the performance of high-speed railway EEW systems is an urgent and important research question.

1.3 Influence of ground-motion attenuation relationships on high-speed railway EEW

High-speed railway EEW exploits the velocity difference between P-waves (primary waves), S-waves (secondary waves), and electromagnetic signals to issue emergency response information before damaging seismic waves reach trains along the affected lines. The performance of EEW is influenced by the adopted ground-motion attenuation relationships.

The EEW process begins with a rapid estimation of earthquake source parameters such as magnitude and hypocentral distance. Based on ground-motion attenuation relationships, the system then generates real-time "seismic intensity distribution maps." Regions for which the predicted peak ground acceleration (PGA) exceeds the warning threshold are identified as alert zones.

Attenuation relationships directly determine the agreement between the "predicted ground-motion field" and the "actual ground-motion field," thereby affecting the rates of missed alarms, false alarms, and the effective warning time window. Sources of error in attenuation relationships include uncertainties in the empirical models themselves and in site-effect parameters (Chen, Hu, & Huo, 1992; Bommer, 2007; Atik, Bommer, Scherbaum, Cotton, & Kuehn, 2010). As empirical models, attenuation relationships contain random error terms and exhibit inherent scatter. The VS30 model—representing the time-averaged shear-wave velocity in the upper 30 m of the subsurface—can underestimate long-period response spectra, introducing errors that may reduce the warning radius or result in missed alerts.

For near-field ground motions of small-to-moderate earthquakes, different attenuation models—such as HDGF and HY99—can yield significantly divergent estimates (Li, Yan, & Pan, 2005). The applicability of each model must therefore be assessed before use. For strong ground motions, attenuation characteristics also vary regionally, with most models being valid only for specific geographical areas (Yu, Li, & Xiao, 2013). Ground-motion attenuation with distance includes both geometric spreading and anelastic attenuation. For earthquakes with the same focal depth, geometric attenuation is consistent across regions, whereas anelastic attenuation varies geographically. In tectonically stable regions, anelastic attenuation is small and the quality factor (Q) is relatively high; in tectonically active regions, anelastic attenuation is larger and Q is lower.

The core contribution of this study is to build upon the high-speed railway EEW system's advantage of aggregating massive multi-source information—including seismic monitoring data, EEW alerts, predicted PGA maps, ground-motion parameters, rapid earthquake

parameter reports, and alarm signals—from the primary line, adjacent lines, neighboring bureaus, and the China Earthquake Network. We propose a new PLUM-based warning and response methodology designed to minimize the impact of errors in ground-motion attenuation relationships, thereby maximizing the effective use of the available seismic information.

2. Application of the PLUM method to high-speed railway earthquake early warning

This study adopts a strategy of "using self-built stations in the field-monitoring tier of the high-speed railway EEW system as the backbone, supplemented by stations from the China Earthquake Network" to design an earthquake early warning and emergency response approach based on the PLUM principle.

2.1 Principle of the PLUM method

In 2013, Hoshiba proposed an emergency response method based on the principle of PLUM (Propagation of Local Undamped Motion) (Hoshiba, 2013). The PLUM method is founded on the Kirchhoff–Fresnel integral theorem and assumes that "seismic waves propagating through bedrock within a suitably sized and shaped region can be regarded as undamped plane waves."

The PLUM method observes ground motions within a designated warning and response region (hereafter "warning region") and uses the maximum PGA observed at any station in that region as the predicted PGA for the entire region. Based on the predicted PGA, the PLUM method issues the corresponding emergency response information for the warning region. As illustrated in Figure 3, because the first station along the incoming wave direction within a warning region will detect seismic signals earliest, the emergency response information issued for that region will precede the arrival of the seismic waves.

2.2 Design of warning regions

In Japan's EEW system, the PLUM method is implemented by dividing the entire country into 188 warning regions based on administrative boundaries (Fujinawa & Noda, 2013). In 2016, Yuki *et al.* (Kodera *et al.*, 2016) used data from the 2016 Kumamoto M7.3 earthquake to test the PLUM method for circular regions with a radius of 30 km, evaluating the timeliness of the response. In 2019, Elizabeth *et al.* (Cochran *et al.*, 2019) analyzed 193 earthquakes of magnitude M3.5 and above occurring between 2012 and 2017, applying the PLUM method to circular regions of various radii and comparing performance across different sizes. Using data from 13 earthquakes with magnitudes above M5.0, the PLUM method successfully detected 12 events without producing any false alarms.

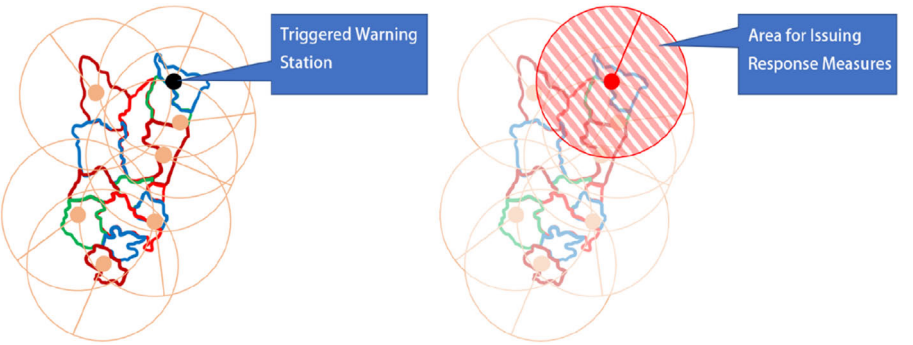

Figure 3. Schematic illustration of the PLUM method. Source(s): Authors' own work

In 2020, (Guan, 2020) applied the PLUM method to data from the 2017 Jiuzhaigou M7.0 earthquake to assess its accuracy. In the same year, (Minson *et al.*, 2020) defined warning regions at three spatial scales—U.S. state boundaries, weather forecast zones, and 50 km square grids—and designed a PLUM-based test system. Using data from the 2019 Ridgecrest M6.4 and M7.1 earthquakes in California, they replayed real-time data streams to evaluate timeliness and accuracy.

In 2021, (Yang, Shan, & Ma, 2021b; Yang, Shan, Ma, & Jing, 2021c) evaluated the timeliness and accuracy of PLUM warnings for the 2021 Fukushima M7.3 earthquake. The same authors (Yang *et al.*, 2021b, c) also tested the method's performance using square grids covering Japan, with grid sizes ranging from 30 to 120 km at 10 km increments, and found that sizes between 60 and 70 km yielded optimal results.

In 2021, (Kilb *et al.*, 2021) conducted experiments to optimize the threshold for triggering PLUM warnings, comparing performance at different thresholds using data from 558 earthquakes and anomalous events in the existing warning system. In 2022, Elizabeth *et al.* (Cochran *et al.*, 2022) sought to optimize warning-region sizes by analyzing 22 M4.4–M7.2 earthquakes along the U.S. West Coast, comparing radii of 20, 60, and 100 km. That same year, (Saunders *et al.*, 2022) evaluated the PLUM method's performance for earthquakes smaller than M4.5, using 432 events of M3.0–M4.0 from the 2021 U.S. West Coast dataset.

2.2.1 Station deployment. To evaluate the PLUM method's performance, an appropriate high-speed railway line was selected as the testbed. The line needed to meet three criteria:

(1) It must already be equipped with a high-speed railway EEW monitoring system.

(2) It must be located in a region frequently affected by seismic events.

(3) The surrounding area must have dense coverage by the national seismic network.

With strong support from relevant organizations and authorities, one line meeting these conditions was selected based on its geographical location, historical earthquake records, and seismic network coverage.

Next, existing stations from the field-monitoring tier of the high-speed railway's EEW system were selected as the backbone. These stations had originally been positioned at intervals of 20–30 km along the railway line (Jin, 2021). It is important to note that, due to practical constraints, this study did not involve site selection, construction, equipment installation, or retrofitting of stations.

Finally, to increase the amount of usable seismic-event data, additional stations from the nearby national seismic network were incorporated as enhancements. The resulting station deployment used for this research is shown in Figure 4.

2.2.2 Geometric shape and layout of warning regions. The effectiveness of the PLUM method depends on the geometric shape and spatial layout of the warning regions. Traditional PLUM implementations use circular, square, or irregularly shaped regions based on administrative boundaries. In the context of high-speed railway EEW, warning regions require more targeted geometric designs. Past implementations have used both administrative-boundary layouts (Fujinawa & Noda, 2013; Minson *et al.*, 2020) and regular geometric grids (Minson *et al.*, 2020; Yang *et al.*, 2021b, c).

For the selected high-speed railway line, this study designed the warning region layout shown in Figure 5, consisting of seven identically shaped regions. These warning regions were arranged

symmetrically on both sides of the railway line. To ensure that seismic network stations were included, the regions were extended 30 km perpendicular to the railway alignment ($h = 30$ km), as illustrated in Figure 6.

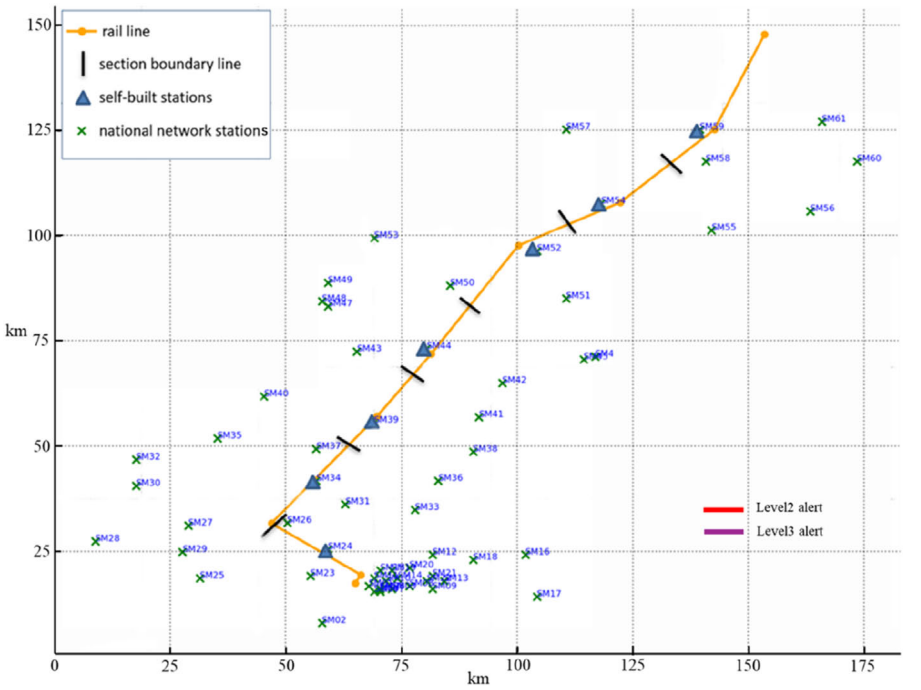

Figure 4. Distribution of railway and seismic stations. Source(s): Authors' own work

2.3 Design of the emergency response information release algorithm

Currently, each self-built station is equipped with a pair of strong-motion seismometers. An alarm is triggered only if both instruments record signals exceeding a predefined threshold (Jin, 2021). For the purpose of verifying the PLUM principle in this study, the configuration is simplified to a single strong-motion seismometer per station.

2.3.1 Mathematical formulation. The fundamental concept of the PLUM method is to assume that seismic waves propagate without attenuation within a designated region, allowing direct prediction of future ground motions based on observed ground-motion data, rather than relying on seismic wave propagation models or source parameters. In presenting the algorithmic framework, this study follows the convention of Ref. Kodera *et al.* (2016) by using real-time seismic intensity to characterize ground motion strength. However, in the subsequent application to high-speed rail earthquake early warning, ground motion acceleration is adopted as the primary metric. Its mathematical expression is given as:

$$I_{pred}^{(k)} = \max\left(Ir_{obs}^{(i)} - F_0^{(i)}\right) + F_0^{(k)}$$

Where i and k denote spatial positions. $I_{pred}^{(k)}$ and $Ir_{obs}^{(i)}$ represent the predicted seismic intensity at point k and the observed seismic intensity at point i, respectively. $F_0^{(k)}$ are the site amplification factors at points i and k.

As illustrated in Figure 7, the basic steps are as follows:

(1) Select prediction point k: Identify the location where the seismic intensity is to be predicted.

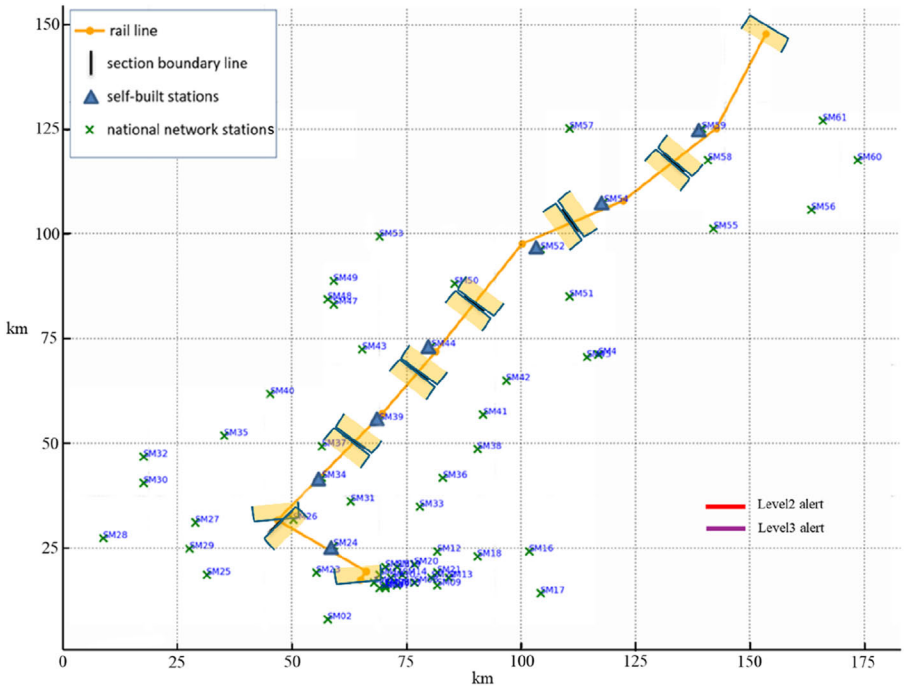

Figure 5. Layout of warning regions. Source(s): Authors' own work

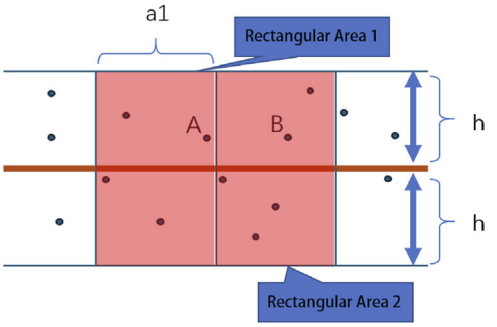

Figure 6. Geometry of warning-region parameters. Source(s): Authors' own work

(2) Search within the neighborhood C_R: Using point k as the center, search within a radius R to locate all observation stations i inside the circle.

(3) Correct the observed values: Since the geological conditions differ among stations, the observed intensity $Ir_{obs}^{(i)}$ must be corrected by removing the local site amplification factor $F_0^{(i)}$ to yield the "true" intensity suitable for propagation.

(4) Propagate to the prediction point: From all nearby stations, select the maximum corrected intensity (a conservative strategy representing the "most hazardous" source). Add the site amplification factor $F_0^{(k)}$ of the prediction point to restore its local geological conditions and obtain the predicted intensity at k.

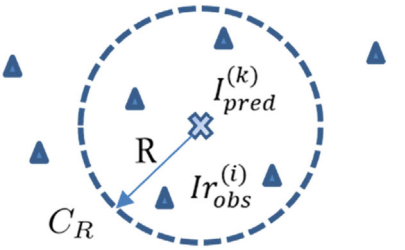

Figure 7. Illustration of the PLUM prediction algorithm. Source(s): Authors' own work

The above constitutes the basic PLUM procedure. In engineering applications, its specific implementation may be adapted to meet operational requirements.

2.3.2 Algorithm description. The focus of this research is the application of PLUM in the context of high-speed railway early warning systems. Internationally, many countries use VS30 as an indicator of site amplification effects (Lü & Zhao, 2007). Given that the foundations along high-speed railway corridors typically consist of stiff soils or bedrock—corresponding to VS30 values ranging from 500 to 800 m/s—and that PLUM-based early warning systems for high-speed rail predefine both the warning region and acceleration thresholds, the normalized error in ground motion estimation is typically less than 5%. Therefore, provided that the regional zoning and threshold design are sufficiently well-calibrated, the influence of local site effects on warning performance can be considered negligible in this application.

In addition, to align with practical engineering applications, this study adopts ground motion acceleration—rather than seismic intensity—as the primary indicator of earthquake severity. This choice reflects the operational reality that seismic stations along high-speed rail corridors directly monitor acceleration time histories, making acceleration-based thresholds more suitable and actionable for real-time decision-making in early warning systems. Accordingly, the PLUM method in this study is simplified to the following formulation:

$$PGA_{pred}^{(k)} = \max\left(Ar_{obs}^{(i)}\right)$$

In this formulation, $PGA_{pred}^{(k)}$ and $Ar_{obs}^{(i)}$ represent the predicted PGA at point *k* and the observed ground motion acceleration at point *i*. For PLUM-based warning information processing, two operational considerations are applied:

(1) The method is only effective if the seismic waves, during propagation, are capable of inducing strong shaking both at the observation point and at the prediction point.

(2) Since P-wave-based EEW performs better for smaller earthquakes, to avoid excessive disruption to railway operations, the system adopts a two-tiered alarm validity rule:

- When a station detects a PGA exceeding 80 gal, a Level-2 alarm is immediately issued for the entire warning region.
- When a station detects a PGA exceeding 120 gal, a Level-3 alarm is issued.

The system receives PGA data from seismic monitoring stations along the high-speed railway and from the broader seismic network. Each station provides a time series representing the recorded acceleration at discrete time points. Alarm decisions are made independently for each warning region. The system updates PGA data every 0.01 s, continuously retrieving the "current" PGA values, and for each region, it extracts the maximum PGA recorded across all its stations at that time to determine whether the threshold is exceeded.

3. Simulation experiments and validation

Due to practical constraints, this study employed simulation experiments to validate the effectiveness of the proposed PLUM-based earthquake early warning and emergency response method for high-speed railways.

A high-speed railway line already equipped with an EEW monitoring system was selected. The test line is located near a seismically active region and is well covered by a dense seismic network, providing abundant recorded data for simulation. The experiments were conducted offline and were completely isolated from the operational system. To avoid confusion between simulation data and real seismic events, all absolute location information of both the earthquakes and the test line was removed, retaining only their relative spatial relationships. Based on this, the emergency-response warning regions were designed.

3.1 Simulation experiment design

If the warning regions are set as rectangles with side lengths of 30 km and 60 km (a1 = a2 = 30 km), as shown in Figure 8, a station (e.g. Station A) located near the boundary of Region 1 might trigger an alarm only for Region 1 when seismic waves arrive. However, the shaking intensity in Region 2 could be similar, and emergency information for Region 2 might only be issued when a more distant station (e.g. Station B) is triggered, reducing the timeliness of warnings for Region 2.

To mitigate this issue, the central lines of the long edges of the rectangles were extended in both directions, transforming the warning regions into adjacent isosceles trapezoids with shared long bases. This design allows neighboring regions to overlap and share stations (Figure 8). If a station in the overlapping area is triggered, emergency response information is issued for both regions simultaneously.

In the proposed dual-trapezoid configuration, the long base a2 is set to 40 km. Historical seismic records from multiple events were used to verify the timeliness of emergency information release, the accuracy of warning levels, and overall system effectiveness.

3.2 Selection of earthquake events and data

To ensure comprehensive testing, 82 earthquake events with magnitudes M5.0–7.0 were selected based on the station–epicenter distance distribution. Sixty-one stations with recorded ground acceleration data were used (Figure 9). The dataset comprised 6,100 station–event records, with epicentral distances predominantly in the range of 100–150 km, a minimum distance of 5 km, and a maximum of 500 km. Each record included three-component acceleration data (east–west, north–south, and vertical) and covered the full time span from before the event to after its conclusion.

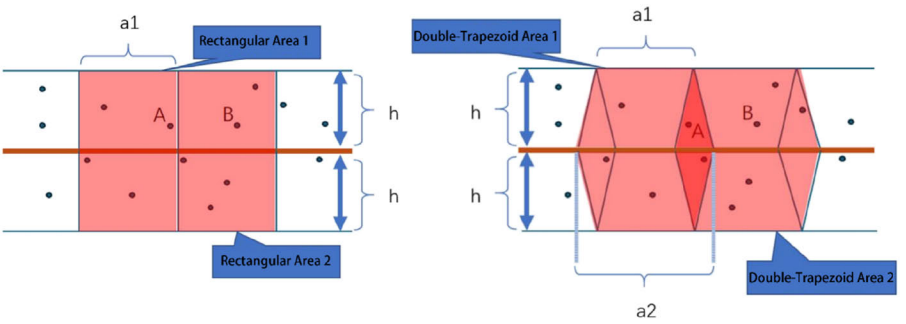

Figure 8. Overlapping double-trapezoid design of warning regions. Source(s): Authors' own work

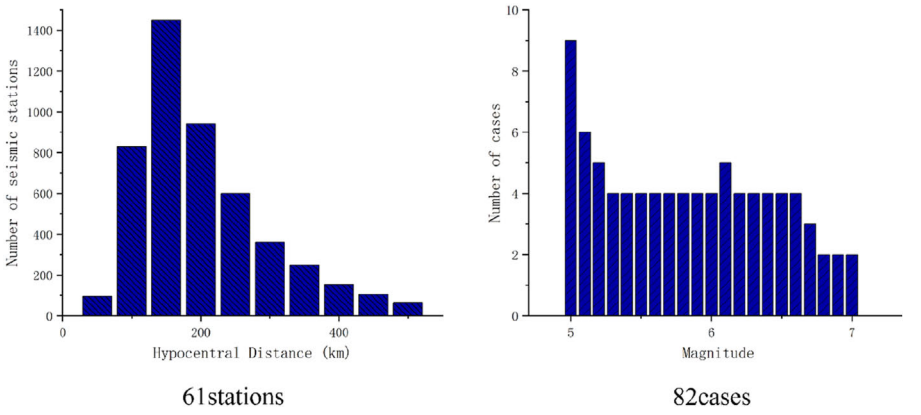

Figure 9. Distribution of seismic stations and earthquake events. Source(s): Authors' own work

4. Results, analysis, and discussion

4.1 Temporal evolution of emergency information in a single trial

A magnitude 5.5 earthquake record, with an epicentral distance of 43 km from the test line, was used. Seven seconds after the earthquake occurred, the first warning region issued a Level-2 emergency message, which was upgraded to Level-3 at 9 seconds. Twelve seconds after the event, the second warning region issued a Level-2 message. As the seismic waves propagated, subsequent regions sequentially issued or updated emergency messages (Figure 10). Figure 10 shows the release process of emergency information, with the first issuance of a Level-2 alarm in each region marked as the reference time point.

4.2 Accuracy analysis

For three events with magnitudes M6.2, 6.3, and 6.4, each warning region was divided into three subregions of 10 km each. The PLUM-based final results were compared with the observed peak ground accelerations (Figure 11):

Results indicated that in all three events, the PLUM method was highly reliable, accurately warning nearly all sections of the railway without any missed alarms.

4.3 Timeliness analysis of warning and response information

4.3.1 Analysis of single earthquake events. Across four earthquake events of varying magnitudes, the timeliness of the PLUM method was compared for regions at different epicentral distances. As shown in Figure 12, we found that particularly in higher-magnitude earthquakes, the PLUM method demonstrated superior timeliness for regions located closer to the epicenter. However, for regions farther from the epicenter, the advantage in timeliness diminished compared to disposal-range algorithms that rely on attenuation models.

4.3.2 Analysis of multiple earthquake events. We further analyzed the performance of the PLUM method in regions within 0–100 km of the epicenter across 82 earthquake events with magnitudes ranging from 5.0 to 7.0. As illustrated in Figure 13, the PLUM method generally exhibited better timeliness in higher-magnitude earthquakes. In large earthquakes with greater rupture areas, the PLUM method was able to provide longer warning

times for regions very close to the epicenter, prior to the arrival of the most destructive seismic waves. This may be attributed to the longer rupture duration of large earthquakes, while the method in this study, tailored for high-speed railway early warning scenarios, employed two relatively low acceleration thresholds for triggering. Conversely, in

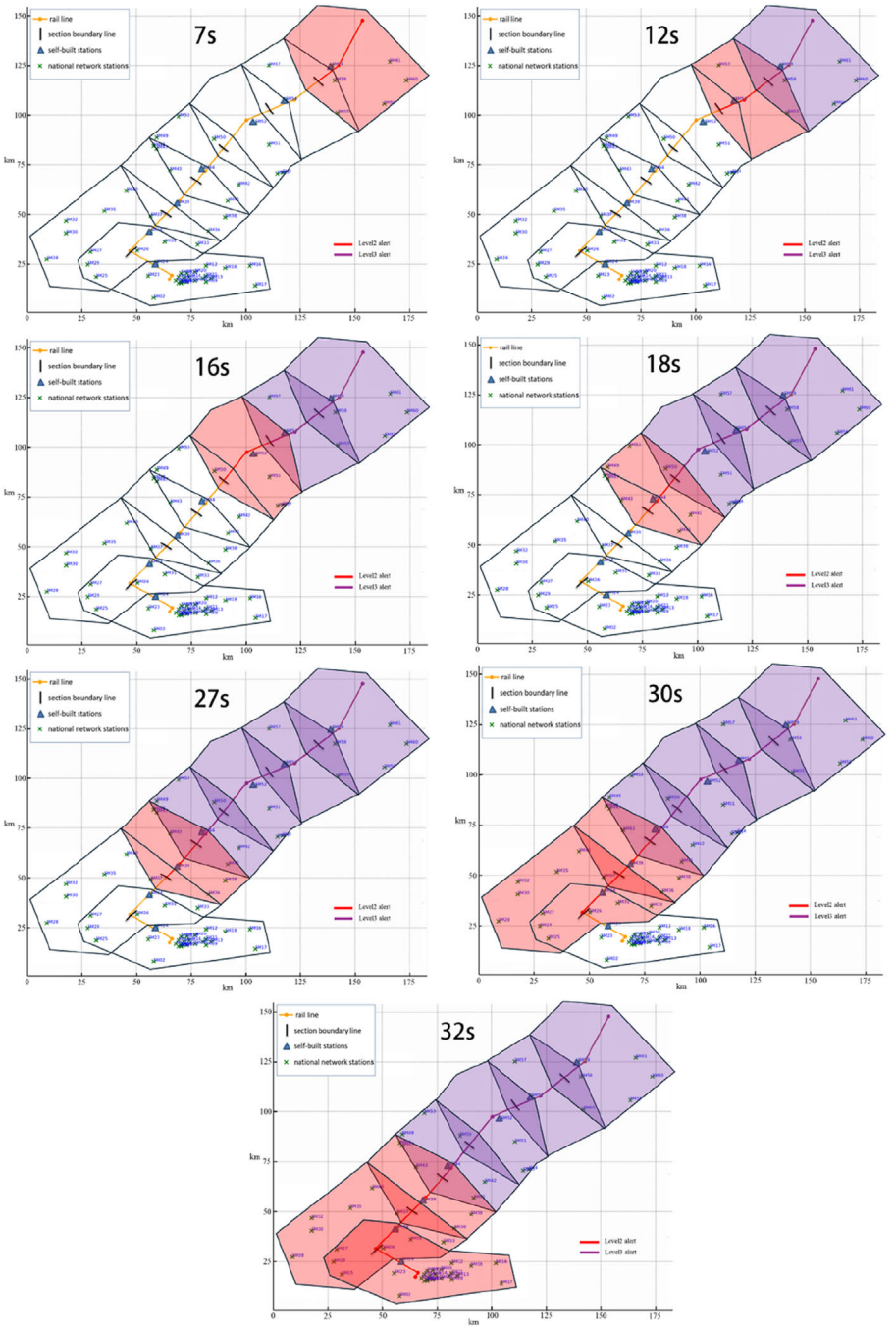

Figure 10. Sequential activation of warning regions. Source(s): Authors' own work

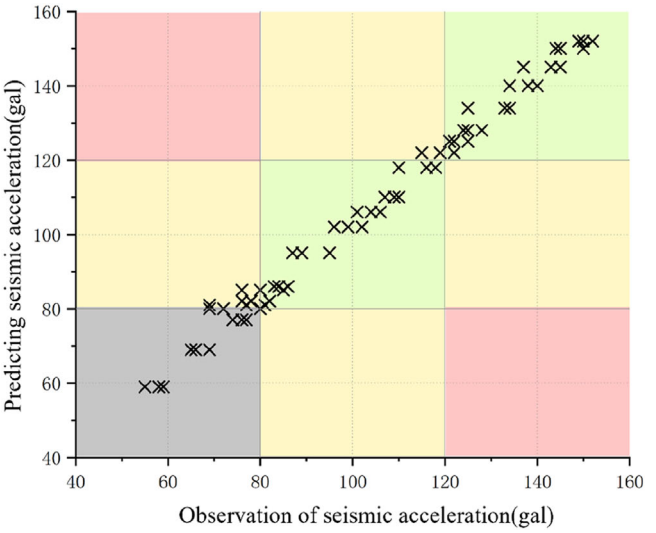

Figure 11. Comparison of predicted and observed PGA. Note(s): *Green:* Alarm issued was exactly correct. *Gray:* No alarm issued, and the threshold was not reached. *Yellow:* Alarm level differed from the expected level by one grade. *Red:* Alarm level differed by two grades. Source(s): Authors' own work

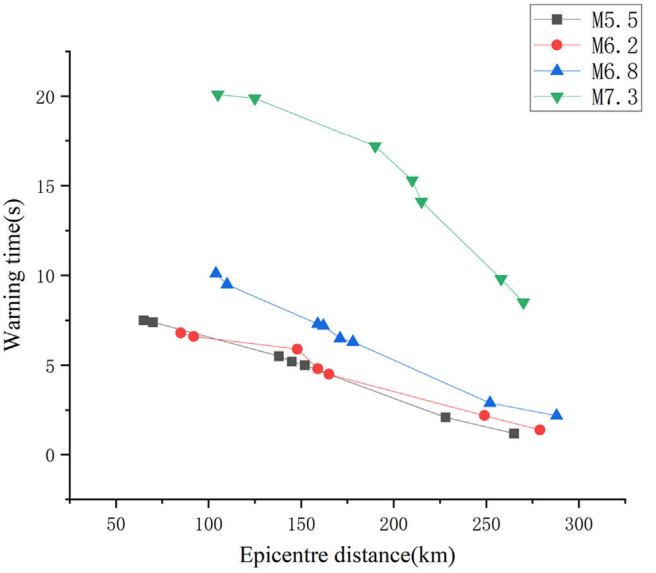

Figure 12. Warning time vs. epicentral distance. Source(s): Authors' own work

lower-magnitude earthquakes, the method showed poorer timeliness for regions with either very small or very large epicentral distances.

As shown in Figure 11, for earthquakes with magnitudes M5.0–7.0 and epicentral distances of 0–100 km, the PLUM method demonstrated robust performance.

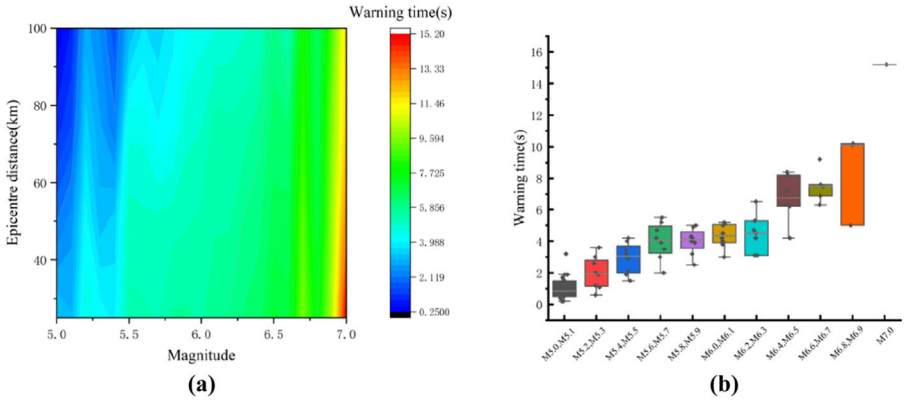

Figure 13. Heatmap and statistical distribution of warning time. Note(s): (a) System performance for all earthquake events within 0–100 km epicentral distance (b) Boxplot of system performance at approximately 25 km epicentral distance. Source(s): Authors' own work

5. Conclusions and outlook

The performance of high-speed railway earthquake early warning systems is significantly influenced by ground-motion attenuation relationships. With increasing integration with the national seismic network, a growing variety of information is now incorporated into the railway early warning monitoring system, enabling the potential application of fundamentally different warning and disposal strategies.

This study proposed a PLUM-based emergency disposal method for high-speed railways, including the design of warning-region geometry and the development of an algorithm for issuing emergency information. Using observational data from 82 earthquake events and a test railway line, we validated the proposed approach through simulation experiments. The results demonstrate that the method successfully issued emergency disposal information across multiple warning regions covering the test line. In many cases, the method achieved excellent timeliness and accuracy, and by incorporating data from national seismic network stations, it has the potential to complement attenuation-based methods such as P-wave early warning in certain earthquake scenarios.

The PLUM-based disposal method holds considerable promise for application in high-speed railway earthquake early warning. Future work should focus on developing a digital simulation environment for more precise modeling of test lines, as well as conducting research to enhance the credibility of simulation results. Additionally, further validation across a broader set of railway lines and earthquake events will be essential to improving the regional applicability of the proposed method.

References

Atik, L., Bommer, J., Scherbaum, F., Cotton, F., & Kuehn, N. (2010). The variability of ground-motion prediction models and its components. *Seismological Research Letters*, *81*(5), 794–801. doi: 10.1785/gssrl.81.5.794.

Bommer, J., & Abrahamson, N. A. (2007). Why do modern probabilistic seismic-hazard analyses often lead to increased hazard estimates?. *Bulletin of the Seismological Society of America*, *96*(6), 1967–1977. doi: 10.1785/0120060043.

Chen, H., Hu, Y., & Huo, J. (1992). Influence of uncertainty in attenuation relation coefficients on seismic hazard analysis results. *North China Earthquake Sciences*, *10*(4), 49–54.

China Earthquake Networks Center (2025). Introduction to China's seismic observation network. Available from: https://data.earthquake.cn/datashare/website/data/datashare_network_china.jsp (accessed 29 July 2025).

Cochran, E. S., Bunn, J., Minson, S. E., Baltay, A. S., Kilb, D. L., Kodera, Y., & Hoshiba, M. (2019). Event detection performance of the PLUM earthquake early warning algorithm in Southern California. *Bulletin of the Seismological Society of America*, *109*(4), 1524–1541. doi: 10.1785/0120180326.

Cochran, E. S., Saunders, J. K., Minson, S. E., Bunn, J., Baltay, A., Kilb, D., … Kodera, Y. (2022). Alert optimization of the PLUM earthquake early warning algorithm for the Western United States. *Bulletin of the Seismological Society of America*, *112*(2), 803–819. doi: 10.1785/0120210259.

Fujinawa, Y., & Noda, Y. (2013). Japan's earthquake early warning system on 11 March 2011: Performance, shortcomings, and changes. *Earthquake Spectra*, *29*(1S), 341–368. doi: 10.1193/1.4000127.

Guan, S. (2020). Research on the PLUM method in earthquake early warning. [Master's thesis, Institute of Engineering Mechanics, China Earthquake Administration].

Guo, Q. (2016). Development of earthquake monitoring and early warning signal interface unit for high-speed railways. *China Railway Science*, *37*(3), 138–144.

Hoshiba, M. (2013). Real-time prediction of ground motion by Kirchhoff–Fresnel boundary integral equation method: Extended front detection method for earthquake early warning. *Journal of Geophysical Research: Solid Earth*, *118*(3), 1038–1050. doi: 10.1002/jgrb.50119.

Hu, Z. (2016). Design and application of signal interface unit for high-speed railway earthquake monitoring and early warning system. [Master's thesis, China Academy of Railway Sciences].

Hu, Z., & Yang, L. (2024). Research on the application of digital twin technology in high-speed railway EEW systems. *Railway Transport and Economy*, *46*(3), 115–124.

Hu, Z., Liu, Z., & Yang, L. (2016). Research on protection strategies for high-speed railway earthquake early warning. *Railway Communication Signal*, *52*(8), 15–18.

Jiang, W., Ma, L., Ye, Y., Zhang, G., & Shi, J. (2019). Method for extracting railway line feature points for earthquake early warning. *Railway Construction*, *59*(8), 113–116.

Jin, X. (2021). *Earthquake early warning and intensity rapid report: Theory and practice*. Beijing: Science Press (pp. 310–331).

Kilb, D., Bunn, J. J., Saunders, J. K., Cochran, E. S., Minson, S. E., Baltay, A., … Kodera, Y. (2021). The PLUM earthquake early warning algorithm: A retrospective case study of West Coast, USA data. *Journal of Geophysical Research: Solid Earth*, *126*(7), e2020JB021478. doi: 10.1029/2020jb021053.

Kodera, Y., Saitou, J., Hayashimoto, N., Adachi, S., Morimoto, M., Nishimae, Y., & Hoshiba, M. (2016). Earthquake early warning for the 2016 Kumamoto earthquake: Performance evaluation of the current system and next-generation methods of the Japan Meteorological Agency. *Earth, Planets and Space*, *68*(1), 202–215. doi: 10.1186/s40623-016-0567-1.

Li, X., Yan, X., & Pan, H. (2005). Applicability analysis of ground-motion attenuation relationships in near-field motion estimation for small-to-moderate earthquakes. *Earthquake Engineering and Engineering Vibration*, *25*(1), 1–7.

Liu, Z. (2019). Structure and optimization of high-speed railway earthquake early warning system. *Railway Communication Signal*, *55*(z1), 171–175.

Liu, M., Shang, L., & Feng, K. (2021). Research on earthquake early warning and disposal strategy of high-speed railway train operation. *Railway Transport and Economy*, *43*(7), 99–104.

Lü, H., & Zhao, F. (2007). Response spectrum amplification factors for site classification in China. *Acta Seismologica Sinica*, *114*(1), 67–76.

Minson, S. E., Saunders, J. K., Bunn, J. J., Cochran, E. S., Baltay, A. S., Kilb, D. L., … Kodera, Y. (2020). Real-time performance of the PLUM earthquake early warning method during the 2019 M6.4 and 7.1 Ridgecrest, California, earthquakes. *Bulletin of the Seismological Society of America*, *110*(4), 1887–1903. doi: 10.1785/0120200021.

Saunders, J. K., Minson, S. E., Baltay, A. S., Bunn, J. J., Cochran, E. S., Kilb, D. L., … Kodera, Y. (2022). Real-time earthquake detection and alerting behavior of PLUM ground-motion-based early warning in the United States. *Bulletin of the Seismological Society of America*, *112*(5), 2668–2688. doi: 10.1785/0120220022.

TDengine (2023). Single-day access of 500 billion rows/900 GB data: Application of TDengine 3.0 in China Earthquake Networks Center. Available from: https://zhuanlan.zhihu.com/p/658215191 (accessed 29 July 2025).

Xi, N., Wang, L., Ma, L., Yang, L., & Wen, R. (2017). Study on delay characteristics of local earthquake monitoring and early warning in high-speed railway. *World Earthquake Engineering*, *33*(4), 94–103.

Yan, L. (2017). Research on high-speed railway earthquake emergency response system. *Railway Communication Signal*, *53*(1), 79–82.

Yan, L., Yang, L., & Guo, Q. (2016). Design and implementation of railway earthquake monitoring and early warning system based on WebGIS. *Railway Communication Signal*, *52*(2), 81–83.

Yang, L. (2018a). Rapid generation algorithm of emergency information for high-speed railway earthquake early warning system. *China Railway Science*, *39*(3), 125–130.

Yang, L. (2018b). Research on processing platform of seismic intensity information. *Railway Communication Signal*, *54*(11), 1–6.

Yang, L., Yan, L., & Guo, Q. (2015). Research on the application of earthquake monitoring and early warning central system in railways. *Railway Communication Signal*, *51*(12), 60–64.

Yang, L., Liu, Z., Zhang, G., & Hu, Z., (2019). Research on fusion early warning technology of high-speed railway EEW system and seismic networks. *Railway Transport and Economy*, *41*(10), 64–70.

Yang, L., Yan, L., & Zhang, G. (2021a). Research on the design of earthquake early warning emergency response system for urban rail transit. *Railway Transport and Economy*, *43*(7), 118–124.

Yang, L., Shan, Z., Ma, R., & Jing, L. (2021b), "Simulation of the PLUM method during the 2021 Fukushima M7.3 earthquake", *World Earthquake Engineering*, Vol. 37 No. 2, pp. 82-89.

Yang, L., Shan, Z., Ma, R., & Jing, L. (2021c). Influence of the warning area division on the effect of the PLUM method. In *ICHCE and SWIDR 2021* (pp. 32–36).

Yang, L., Gong, Y., Gong, S., Zhou, D., & Zhang, Y. (2022). Overview on risk of earthquake early warning for transportation systems. In *2022 6th International Conference on System Reliability and Safety (ICSRS)* (pp. 226–232). doi: 10.1109/icsrs56243.2022.10067373.

Yang, L., Zhang, G., Hu, Z., & Zhou, D. (2023a), "Research on rapid determination algorithm of seismic intensity information based on measured waveform and its application in railways", *Railway Standard Design*, Vol. 67 No. 2, pp. 155-160.

Yang, L., Zhu, J., & Zhang, X. (2023b). Application of China's high-speed railway earthquake early warning system in Jakarta–Bandung high-speed railway. *China Railway*, *1*(12), 122–129.

Yu, Y., Li, S., & Xiao, L. (2013). Ground-motion attenuation relations for new zoning map compilation. *Technology for Earthquake Disaster Prevention*, *8*(1), 24–33.

Datian Zhou received his Ph. D. degree in Traffic Information Engineering and Control from Beijing Jiaotong University. He was a visiting scholar in Ecole Centale de Paris in 2015. His research interests include analyzing algorithm intensive critical system, such as Earthquake Early Warning Algorithm. He has been involved in several projects of Center of National Railway Intelligent Transportation System Engineering and Technology.

Corresponding author
Datian Zhou can be contacted at: dtzhou@bjtu.edu.cn